Electronic Supplementary Material for

Soft network materials with isotropic negative Poisson's ratios over large strains

Jianxing Liu[1] and Yihui Zhang[1,*]

[1] Center for Mechanics and Materials; Center for Flexible Electronics Technology; AML, Department of Engineering Mechanics; Tsinghua University, Beijing 100084, China

Correspondence and requests for materials should be addressed to Y.Z. (email: yihuizhang@tsinghua.edu.cn).

Keywords: Poisson's ratio; Bioinspired designs; Lattice; Modeling; Shape memory effect

Note I: Analytic solutions to the linear Poisson's ratio

For a planar beam with an arbitrary curvy shape, as shown in **Fig. S4a**, a curvilinear coordinate (S) can be adopted to describe the shape of its central axis in the Cartesian coordinates (X, Y) with the origin at the left end of the microstructure, i.e.,

$$X = X(S),\ Y = Y(S)\,. \tag{S1}$$

Consider the simply supported conditions in which the microstructure is subject to a horizontal force N_0 at the right end and moments M_A and M_B at the left and right ends respectively, as shown in **Fig. S4a**. The axial force N and bending moment M at a cross section S are then related to the internal force N_0 and Q_0 along X and Y directions as

$$\begin{aligned} N(S) &= N_0 \cdot X'(S) + Q_0 \cdot Y'(S)\ , \\ M(S) &= M_A + N_0 \cdot Y(S) - Q_0 \cdot X(S)\ , \end{aligned} \tag{S2}$$

where $X'(S) = \dfrac{\mathrm{d}X(S)}{\mathrm{d}S}$, $Y'(S) = \dfrac{\mathrm{d}Y(S)}{\mathrm{d}S}$ and $Q_0 = \dfrac{M_A - M_B}{L_0}$. For a microstructure with uniform width, its strain energy is given by

$$U = \frac{1}{2E_S A}\int_0^{S_0} N^2 \mathrm{d}S + \frac{1}{2E_S I}\int_0^{S_0} M^2 \mathrm{d}S\,, \tag{S3}$$

where the membrane energy and bending energy are considered; S_0 is the total arc length of the microstructure curve; and $E_S A$ and $E_S I$ are the tensile and bending stiffnesses, respectively. For a microstructure with a reduced width at various turning regions of the curved microstructure, we number the beginning and ending sections of each segment from 1 to n, as shown in **Fig. S4b**. Then the strain energy can be rewritten as

$$\begin{aligned} U = & \frac{1}{2E_S A_1}\sum_{k=0}^{\left[\frac{n-1}{2}\right]}\int_{S_{2k}}^{S_{2k+1}} N^2 \mathrm{d}S + \frac{1}{2E_S A_2}\sum_{k=0}^{\left[\frac{n-2}{2}\right]}\int_{S_{2k+1}}^{S_{2k+2}} N^2 \mathrm{d}S \\ & + \frac{1}{2E_S I_1}\sum_{k=0}^{\left[\frac{n-1}{2}\right]}\int_{S_{2k}}^{S_{2k+1}} M^2 \mathrm{d}S + \frac{1}{2E_S I_2}\sum_{k=0}^{\left[\frac{n-2}{2}\right]}\int_{S_{2k+1}}^{S_{2k+2}} M^2 \mathrm{d}S\ , \end{aligned} \tag{S4}$$

where A_1 and E_1 are area and inertia moment of section 1 (with initial width) respectively, while A_2 and E_2 are used for section 2 with a reduced width. Substitution of Eq. (S2) into Eq.

(S4) gives the strain energy as

$$
\begin{aligned}
U = & \frac{L_0}{2E_S A_1}(\beta_1^1 \cdot N_0^2 + \beta_2^1 \cdot N_0 \frac{M_A - M_B}{L_0} + \beta_3^1 \cdot \frac{M_A^2 + M_B^2 - 2M_A M_B}{L_0^2}) + \frac{L_0}{2E_S A_2}(\beta_1^2 \cdot N_0^2 \\
& + \beta_2^2 \cdot N_0 \frac{M_A - M_B}{L_0} + \beta_3^2 \cdot \frac{M_A^2 + M_B^2 - 2M_A M_B}{L_0^2}) + \frac{L_0}{2E_S I_1}[\beta_4^1 \cdot M_A^2 + \beta_5^1 \cdot (N_0 L_0)^2 \\
& + \beta_6^1 \cdot (M_A^2 + M_B^2 - 2M_A M_B) + \beta_7^1 \cdot M_A (N_0 L_0) + \beta_8^1 \cdot M_A (M_A - M_B) \\
& + \beta_9^1 (N_0 L_0)(M_A - M_B)] + \frac{L_0}{2E_S I_2}[\beta_4^2 \cdot M_A^2 + \beta_5^2 \cdot (N_0 L_0)^2 + \beta_6^2 \cdot (M_A^2 + M_B^2 - 2M_A M_B) \\
& + \beta_7^2 \cdot M_A (N_0 L_0) + \beta_8^2 \cdot M_A (M_A - M_B) + \beta_9^2 (N_0 L_0)(M_A - M_B)] \ ,
\end{aligned}
\tag{S5}
$$

where

$$
\begin{aligned}
& \beta_1^1 = \frac{1}{L_0} \sum_{k=0}^{\left[\frac{n-1}{2}\right]} \int_{S_{2k}}^{S_{2k+1}} [X'(S)]^2 \mathrm{d}S && \beta_1^2 = \frac{1}{L_0} \sum_{k=0}^{\left[\frac{n-2}{2}\right]} \int_{S_{2k+1}}^{S_{2k+2}} [X'(S)]^2 \mathrm{d}S \\
& \beta_2^1 = \frac{2}{L_0} \sum_{k=0}^{\left[\frac{n-1}{2}\right]} \int_{S_{2k}}^{S_{2k+1}} X'(S) Y'(S) \mathrm{d}S && \beta_2^2 = \frac{2}{L_0} \sum_{k=0}^{\left[\frac{n-2}{2}\right]} \int_{S_{2k+1}}^{S_{2k+2}} X'(S) Y'(S) \mathrm{d}S \\
& \beta_3^1 = \frac{1}{L_0} \sum_{k=0}^{\left[\frac{n-1}{2}\right]} \int_{S_{2k}}^{S_{2k+1}} [Y'(S)]^2 \mathrm{d}S && \beta_3^2 = \frac{1}{L_0} \sum_{k=0}^{\left[\frac{n-2}{2}\right]} \int_{S_{2k+1}}^{S_{2k+2}} [Y'(S)]^2 \mathrm{d}S \\
& \beta_4^1 = \frac{1}{L_0} \sum_{k=0}^{\left[\frac{n-1}{2}\right]} \int_{S_{2k}}^{S_{2k+1}} \mathrm{d}S && \beta_4^2 = \frac{1}{L_0} \sum_{k=0}^{\left[\frac{n-2}{2}\right]} \int_{S_{2k+1}}^{S_{2k+2}} \mathrm{d}S \\
& \beta_5^1 = \frac{1}{L_0^3} \sum_{k=0}^{\left[\frac{n-1}{2}\right]} \int_{S_{2k}}^{S_{2k+1}} [Y(S)]^2 \mathrm{d}S && \beta_5^2 = \frac{1}{L_0^3} \sum_{k=0}^{\left[\frac{n-2}{2}\right]} \int_{S_{2k+1}}^{S_{2k+2}} [Y(S)]^2 \mathrm{d}S \\
& \beta_6^1 = \frac{1}{L_0^3} \sum_{k=0}^{\left[\frac{n-1}{2}\right]} \int_{S_{2k}}^{S_{2k+1}} [X(S)]^2 \mathrm{d}S && \beta_6^2 = \frac{1}{L_0^3} \sum_{k=0}^{\left[\frac{n-2}{2}\right]} \int_{S_{2k+1}}^{S_{2k+2}} [X(S)]^2 \mathrm{d}S \\
& \beta_7^1 = \frac{2}{L_0^2} \sum_{k=0}^{\left[\frac{n-1}{2}\right]} \int_{S_{2k}}^{S_{2k+1}} Y(S) \mathrm{d}S && \beta_7^2 = \frac{2}{L_0^2} \sum_{k=0}^{\left[\frac{n-2}{2}\right]} \int_{S_{2k+1}}^{S_{2k+2}} Y(S) \mathrm{d}S \\
& \beta_8^1 = \frac{-2}{L_0^2} \sum_{k=0}^{\left[\frac{n-1}{2}\right]} \int_{S_{2k}}^{S_{2k+1}} X(S) \mathrm{d}S && \beta_8^2 = \frac{-2}{L_0^2} \sum_{k=0}^{\left[\frac{n-2}{2}\right]} \int_{S_{2k+1}}^{S_{2k+2}} X(S) \mathrm{d}S \\
& \beta_9^1 = \frac{-2}{L_0^3} \sum_{k=0}^{\left[\frac{n-1}{2}\right]} \int_{S_{2k}}^{S_{2k+1}} X(S) Y(S) \mathrm{d}S \ , && \beta_9^2 = \frac{-2}{L_0^3} \sum_{k=0}^{\left[\frac{n-2}{2}\right]} \int_{S_{2k+1}}^{S_{2k+2}} X(S) Y(S) \mathrm{d}S \ ,
\end{aligned}
\tag{S6}
$$

are dimensionless parameters depending only on the shape of microstructure; the superscript number of β indicates the corresponding section; L_0 is span between the two ends of microstructure. In the condition of infinitesimal deformations, the relationship between the normalized displacements and loads can be then obtained from Eq. (S5) as

$$\begin{Bmatrix} \bar{u} \\ \omega_A \\ \omega_B \end{Bmatrix} = \begin{bmatrix} \begin{array}{l} \frac{\bar{w}_2^2}{12}(\frac{1}{q}\beta_1^{(2)} + \beta_1^{(1)}) \\ +(\frac{1}{q^3}\beta_5^{(2)} + \beta_5^{(1)}) \end{array} & \begin{array}{l} \frac{\bar{w}_2^2}{24}(\frac{1}{q}\beta_2^{(2)} + \beta_2^{(1)}) + \frac{1}{2}(\frac{1}{q^3}\beta_7^{(2)} \\ +\beta_7^{(1)}) + \frac{1}{2}(\frac{1}{q^3}\beta_9^{(2)} + \beta_9^{(1)}) \end{array} & \begin{array}{l} -\frac{\bar{w}_2^2}{24}(\frac{1}{q}\beta_2^{(2)} + \beta_2^{(1)}) \\ -\frac{1}{2}(\frac{1}{q^3}\beta_9^{(2)} + \beta_9^{(1)}) \end{array} \\ \begin{array}{l} \frac{\bar{w}_2^2}{24}(\frac{1}{q}\beta_2^{(2)} + \beta_2^{(1)}) \\ +\frac{1}{2}(\frac{1}{q^3}\beta_7^{(2)} + \beta_7^{(1)}) \\ +\frac{1}{2}(\frac{1}{q^3}\beta_9^{(2)} + \beta_9^{(1)}) \end{array} & \begin{array}{l} \frac{\bar{w}_2^2}{12}(\frac{1}{q}\beta_3^{(2)} + \beta_3^{(1)}) + (\frac{1}{q^3}\beta_4^{(2)} \\ +\beta_4^{(1)}) + (\frac{1}{q^3}\beta_6^{(2)} + \beta_6^{(1)}) \\ +(\frac{1}{q^3}\beta_8^{(2)} + \beta_8^{(1)}) \end{array} & \begin{array}{l} -\frac{\bar{w}_2^2}{12}(\frac{1}{q}\beta_3^{(2)} + \beta_3^{(1)}) - (\frac{1}{q^3}\beta_6^{(2)} \\ +\beta_6^{(1)}) - \frac{1}{2}(\frac{1}{q^3}\beta_8^{(2)} + \beta_8^{(1)}) \end{array} \\ \begin{array}{l} -\frac{\bar{w}_2^2}{24}(\frac{1}{q}\beta_2^{(2)} + \beta_2^{(1)}) \\ -\frac{1}{2}(\frac{1}{q^3}\beta_9^{(2)} + \beta_9^{(1)}) \end{array} & \begin{array}{l} -\frac{\bar{w}_2^2}{12}(\frac{1}{q}\beta_3^{(2)} + \beta_3^{(1)}) - (\frac{1}{q^3}\beta_6^{(2)} \\ +\beta_6^{(1)}) - \frac{1}{2}(\frac{1}{q^3}\beta_8^{(2)} + \beta_8^{(1)}) \end{array} & \begin{array}{l} -\frac{\bar{w}_2^2}{12}(\frac{1}{q}\beta_3^{(2)} + \beta_3^{(1)}) \\ +(\frac{1}{q^3}\beta_6^{(2)} + \beta_6^{(1)}) \end{array} \end{bmatrix} \bullet \begin{Bmatrix} \bar{N}_0 \\ \bar{M}_A \\ \bar{M}_B \end{Bmatrix}, \tag{S7}$$

with

$$\bar{u} = \frac{u}{L_0};\ \bar{w} = \frac{w}{L_0};\ \bar{N}_0 = \frac{N_0 L_0^2}{E_S I_1};\ \bar{M}_A = \frac{M_A L_0}{E_S I_1};\ \bar{M}_B = \frac{M_B L_0}{E_S I_1}, \tag{S8}$$

where u is the displacement at the right end along the direction of N_0; ω_A and ω_B are the rotational angles at the left and right ends, respectively; w_2 is the reduced width of microstructure, and the width ratio is $q = w_2/w_1$.

For infinitesimal deformations, a triangular network material under horizontal stretching is taken as an example to derive the Poisson's ratio and elastic modulus. Two representative unit cells with different configurations are analyzed, as shown in **Fig. S4c**. According to the static equilibrium of the unit cell, the inner force $\bar{N}_i$ (with i denoting the different microstructures of a unit cell, and i = 1 for the horizontal microstructure), the bending moments $\bar{M}_{iA}$ and $\bar{M}_{iB}$, and the external loading satisfy the following relations:

$$\sqrt{3}\bar{N}_3 + \sqrt{3}\bar{N}_2 + (\bar{M}_{3A} - \bar{M}_{3B}) - (\bar{M}_{2A} - \bar{M}_{2B}) = 0, \tag{S9}$$

$$2(\bar{M}_{1A} - \bar{M}_{1B}) + (\bar{M}_{2A} - \bar{M}_{2B}) - \sqrt{3}\bar{N}_2 = 0, \tag{S10}$$

$$\sigma_1 = \frac{4\bar{N}_1 + \bar{N}_3 + \bar{N}_2 - \sqrt{3}(\bar{M}_{3A} - \bar{M}_{3B}) + \sqrt{3}(\bar{M}_{2A} - \bar{M}_{2B})}{2\sqrt{3}\frac{A_2}{\bar{w}_2}(\frac{L_0^2}{E_S I_2})}, \tag{S11}$$

$$(\bar{M}_{1A} - \bar{M}_{1B}) + (\bar{M}_{2A} - \bar{M}_{2B}) + (\bar{M}_{3A} - \bar{M}_{3B}) = 0, \tag{S12}$$

where σ_x is the effective stress of the triangular lattice along horizontal direction. According to the deformation compatibility in the periodical lattices, the angle between the tangent lines of different microstructures keeps unchanged during the deformation. Then the unit cells should also satisfy the geometric relations given by

$$\begin{cases} \bar{u}_2 - \bar{u}_1 = \frac{1}{\sqrt{3}}(\omega_{3A} + \omega_{2B} - \omega_{1A} - \omega_{3B}) \\ \bar{u}_3 - \bar{u}_1 = \frac{1}{\sqrt{3}}(\omega_{3A} + \omega_{2B} - \omega_{2A} - \omega_{1B}) \end{cases} \text{and} \begin{cases} \bar{u}_2 - \bar{u}_1 = \frac{1}{\sqrt{3}}(\omega_{1B} + \omega_{3A} - \omega_{2A} - \omega_{3B}) \\ \bar{u}_3 - \bar{u}_1 = \frac{1}{\sqrt{3}}(\omega_{2B} + \omega_{1A} - \omega_{2A} - \omega_{3B}) \end{cases}, \tag{S13}$$

$$\omega_{1A} + \omega_{2A} + \omega_{3A} + \omega_{1B} + \omega_{2B} + \omega_{3B} = 0. \tag{S14}$$

The effective strain of the lattice material defined as the percentage of elongation is equal to the unit cell, and can be expressed as

$$\varepsilon_1 = \bar{u}_1. \tag{S15}$$

The constitutive relation of the microstructure, Eq. (S7), can be re-written in the form of a stiffness matrix $[d_{ij}]$ for simplify, as given by

$$\begin{bmatrix} \bar{N}_1 & \bar{N}_2 & \bar{N}_3 \\ \bar{M}_{1A} & \bar{M}_{2A} & \bar{M}_{3A} \\ \bar{M}_{1B} & \bar{M}_{2B} & \bar{M}_{3B} \end{bmatrix} = \begin{bmatrix} d_{11} & d_{12} & d_{13} \\ d_{12} & d_{22} & d_{23} \\ d_{13} & d_{23} & d_{33} \end{bmatrix} \bullet \begin{bmatrix} \bar{u}_1 & \bar{u}_2 & \bar{u}_3 \\ \omega_{1A} & \omega_{2A} & \omega_{3A} \\ \omega_{1B} & \omega_{2B} & \omega_{3B} \end{bmatrix}. \tag{S16}$$

According to Eqs. (S9) - (S16), an analytic solution of the Poisson's ratio and elastic modulus for triangular network materials with arbitrarily shaped microstructures can be obtained as

$$\nu = \frac{2(d_{12} - d_{13})^2 - (d_{11} - d_{22} + 2d_{23} - d_{33})(d_{22} - 2d_{23} + d_{33})}{2(d_{12} - d_{13})^2 - (d_{22} - 2d_{23} + d_{33})(3d_{11} + d_{22} - 2d_{23} + d_{33})}, \tag{S17}$$

$$E = \frac{2\sqrt{3}(d_{11} + d_{22} - 2d_{23} + d_{33})[-(d_{12} - d_{13})^2 + d_{11}(d_{22} - 2d_{23} + d_{33})]E_s I_2 \bar{w}_2}{[-2(d_{12} - d_{13})^2 + (d_{22} - 2d_{23} + d_{33})(3d_{11} + d_{22} - 2d_{23} + d_{33})]A_2 L_0^2}. \tag{S18}$$

These solutions are useful for the deterministic design of network materials to achieve desired mechanical properties. Then we consider a specific zigzag microstructure whose shape can be described as

$$\begin{cases} y = kx & (0 \le x < \frac{L_0}{4}) \\ y = -kx + k\frac{L_0}{2} & (\frac{L_0}{4} \le x < \frac{3L_0}{4}) \\ y = kx - kL_0 & (\frac{3L_0}{4} \le x \le L_0) \end{cases}, \tag{S19}$$

for a single unit. Then the dimensionless parameters of β can be derived as

$$\begin{aligned}
&\beta_1^{(1)} = \frac{1-r}{\sqrt{1+k^2}},\ \beta_2^{(1)} = 0,\ \beta_3^{(1)} = \frac{k^2(1-r)}{\sqrt{1+k^2}},\ \beta_4^{(1)} = \sqrt{1+k^2}(1-r), \\
&\beta_5^{(1)} = \frac{k^2\sqrt{1+k^2}}{48}(1-r)^3,\ \beta_6^{(1)} = \frac{\sqrt{1+k^2}}{48}(16-15r-r^3),\ \beta_7^{(1)} = 0, \\
&\beta_8^{(1)} = \sqrt{1+k^2}(r-1),\ \beta_9^{(1)} = \frac{k\sqrt{1+k^2}}{16}(1-r)^2,\ \beta_1^{(2)} = \frac{r}{\sqrt{1+k^2}},\ \beta_2^{(2)} = 0, \\
&\beta_3^{(2)} = \frac{k^2 r}{\sqrt{1+k^2}},\ \beta_4^{(2)} = \sqrt{1+k^2}r,\ \beta_5^{(2)} = \frac{k^2\sqrt{1+k^2}}{48}(3r-3r^2+r^3), \\
&\beta_6^{(2)} = \frac{\sqrt{1+k^2}}{48}(15r+r^3),\ \beta_7^{(2)} = 0,\ \beta_8^{(2)} = -\sqrt{1+k^2}r,\ \beta_9^{(1)} = \frac{k\sqrt{1+k^2}}{16}(2r-r^2).
\end{aligned} \tag{S20}$$

Based on Eqs. (S7), (S16) and (S17), the analytic solution of Poisson's ratio for the triangular network materials with a single zigzag microstructure can be obtained. When the weakened segments are much narrower than the other segments, i.e., $q \to 0$, the strain energy of the wider segments can be neglected, leading to a simplified solution of Poisson's ratio:

$$\nu = -\frac{18 + 2k^2\left(r^2 - 3r + 3\right)^2 - r\left(18 + 2r^3 - 6r^2 + 3r\right)}{2k^2\left(r^2 - 3r + 3\right)^2 + 3\left(2r^4 - 6r^3 + 9r^2 - 6r + 6\right)}. \tag{S21}$$

Another limiting condition involves the network design with uniform width, i.e., q = 1. In this case, the solution of Poisson's ratio becomes

$$\nu = \frac{-\left(1+2k^2\right)\left(k+k^3\right)^2 + 8\left(4+2k^2-k^4+k^6\right)\overline{w}^2 + 32\left(-1+k^2\right)\overline{w}^4}{\left(15+2k^2\right)\left(k+k^3\right)^2 + 8\left(1+k^2\right)\left(12+2k^2+3k^4\right)\overline{w}^2 + 32\left(1+3k^2\right)\overline{w}^4}. \tag{S22}$$

where $\overline{w} = \overline{w}_2$. For zigzag microstructures with multiple unit cells (i.e., periodicity n_T), the shape of microstructure can be described as

$$\begin{cases} y = kx - k(m\dfrac{L_0}{n_T}) & (m\dfrac{L_0}{n_T} \le x < \dfrac{L_0}{4n_T} + m\dfrac{L_0}{n_T}) \\ y = -kx + k(\dfrac{L_0}{2n_T} + m\dfrac{L_0}{n_T}) & (\dfrac{L_0}{4n_T} + m\dfrac{L_0}{n_T} \le x < \dfrac{3L_0}{4n_T} + m\dfrac{L_0}{n_T}) \\ y = kx - k(m\dfrac{L_0}{n_T} + \dfrac{L_0}{n_T}) & (\dfrac{3L_0}{4n_T} + m\dfrac{L_0}{n_T} \le x \le \dfrac{L_0}{n_T} + m\dfrac{L_0}{n_T}) \end{cases}, \tag{S23}$$

where $m \in [0,\ n_T - 1]$. The solution of Poisson's ratio is given by

$$\nu = \frac{-\left(k+k^3\right)^2\left(9+2k^2-8n_T^2\right)+8\left(1+k^2\right)\left(-2k^2+k^4+4n_T^2\right)\overline{w}^2+32\left(-1+k^2\right)\overline{w}^4}{\left(k+k^3\right)^2\left(-9+2k^2+24n_T^2\right)+8\left(1+k^2\right)\left(2k^2+3k^4+12n_T^2\right)\overline{w}^2+32\left(1+3k^2\right)\overline{w}^4}. \tag{S24}$$

Using a similar approach, the analytic solution of the Poisson's ratio can be also obtained for the honeycomb network material. For $q \to 0$, it is given by

$$\nu = -\frac{k^2(3+(-3+r)r)-r^2-3}{3k^2(3+(-3+r)r)+r^2+3}. \tag{S25}$$

For q = 1, the Poisson's ratio is written as

$$\nu = -\frac{\left(1+k^2\right)^2\left(-192n_T{}^4+k^2\left(9+16n_T{}^2\right)\right)+16\left(1+k^2\right)n_T{}^2\left(k^4+4\left(1-3k^2\right)n_T{}^2\right)\overline{w}^2+64k^2n_T{}^4\overline{w}^4}{3\left(1+k^2\right)^2\left(64n_T{}^4+k^2\left(-3+16n_T{}^2\right)\right)+48\left(1+k^2\right)n_T{}^2\left(k^4+4\left(1+k^2\right)n_T{}^2\right)\overline{w}^2+192k^2n_T{}^4\overline{w}^4}. \tag{S26}$$

Figure S1. Comparison between experimental images and FEA predictions for the deformation sequences of the entire samples in **Fig. 2a, b,** and **c**. Scale bars, 5 cm.

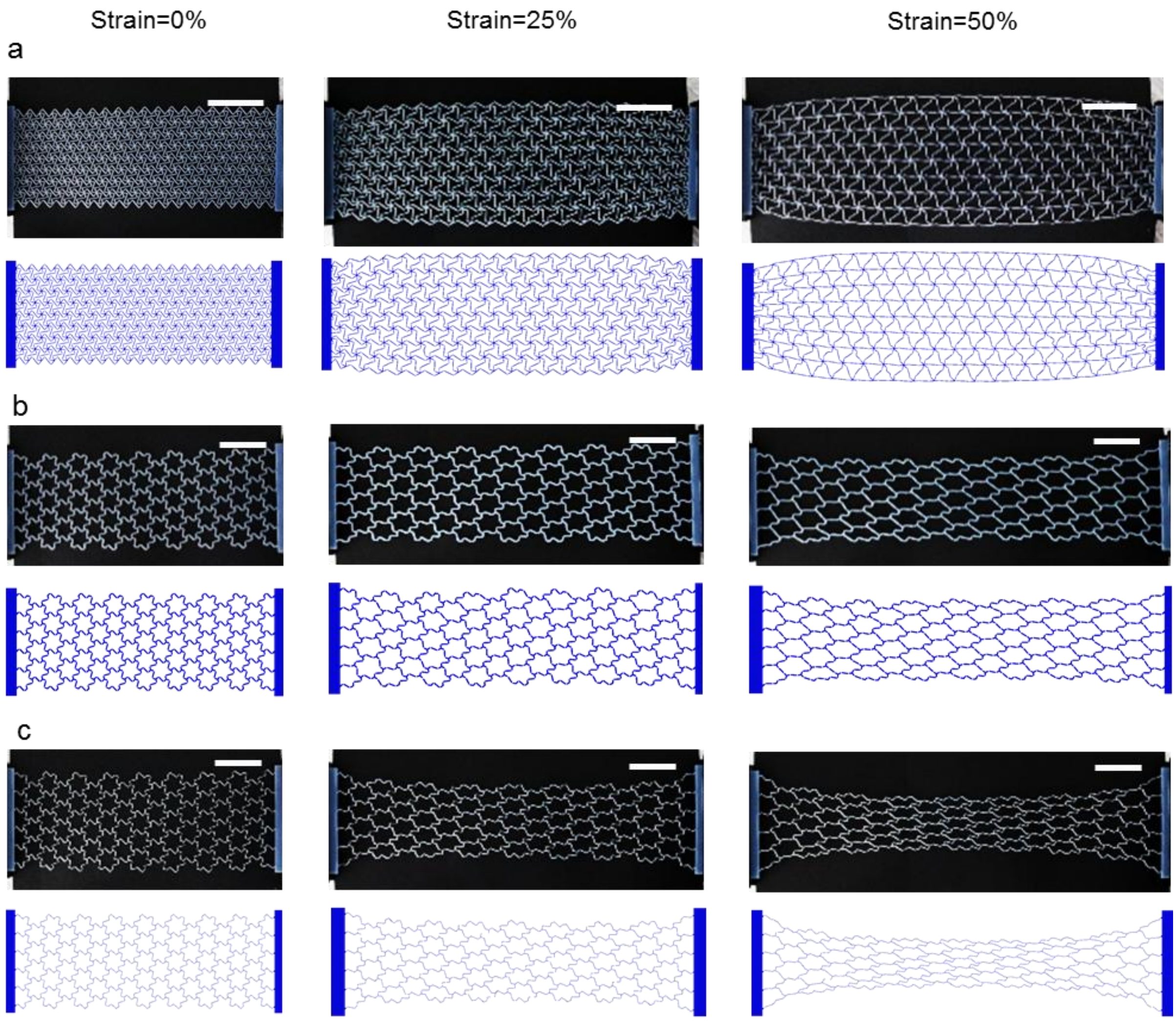

Figure S2. FEA results on the distribution of maximum principal strain for the three examples of triangular and honeycomb network materials in **Fig. 2a**, **b**, and **c**, under uniaxial stretching (25% and 50%).

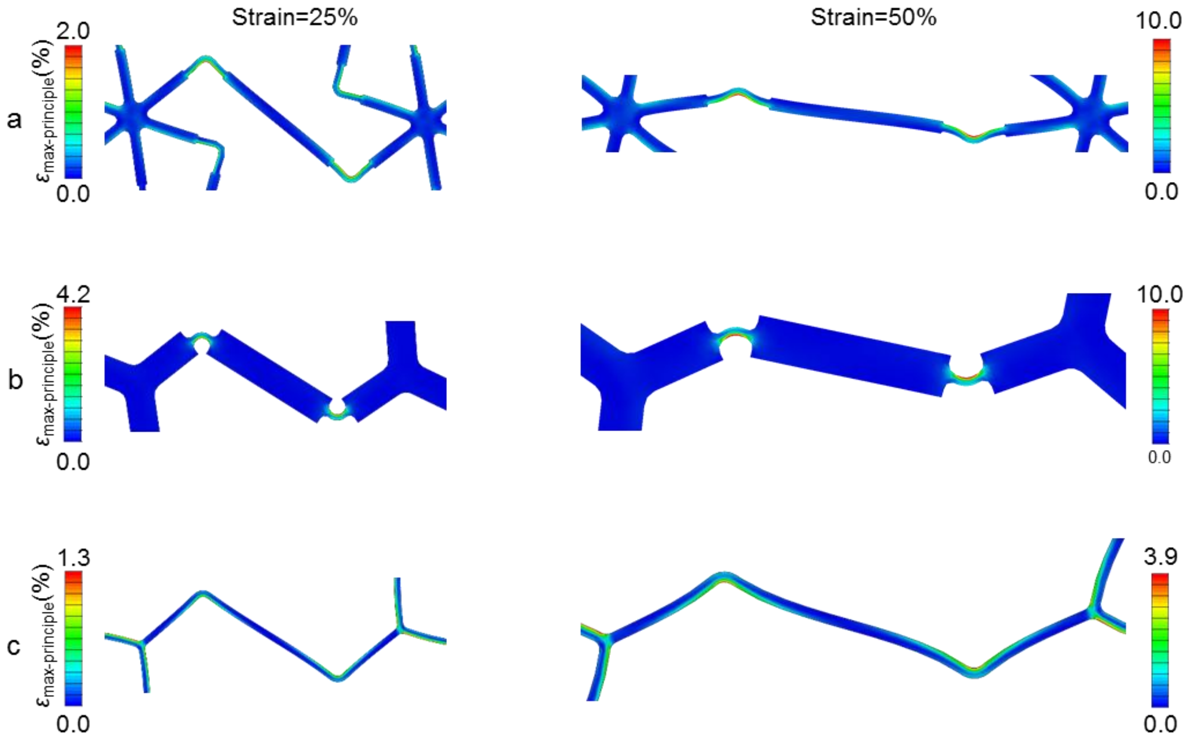

Figure S3. Results of the Poisson's ratio based on two different definitions ($v' = -\, d\varepsilon_y/d\varepsilon_x$ and $v = -\, \varepsilon_y/\varepsilon_x$), for the three network materials in **Fig. 2a**, **b**, and **c**. The dashlines denote the critical strain (ε_{cr}) of the zigzag microstructure of different lattice materials.

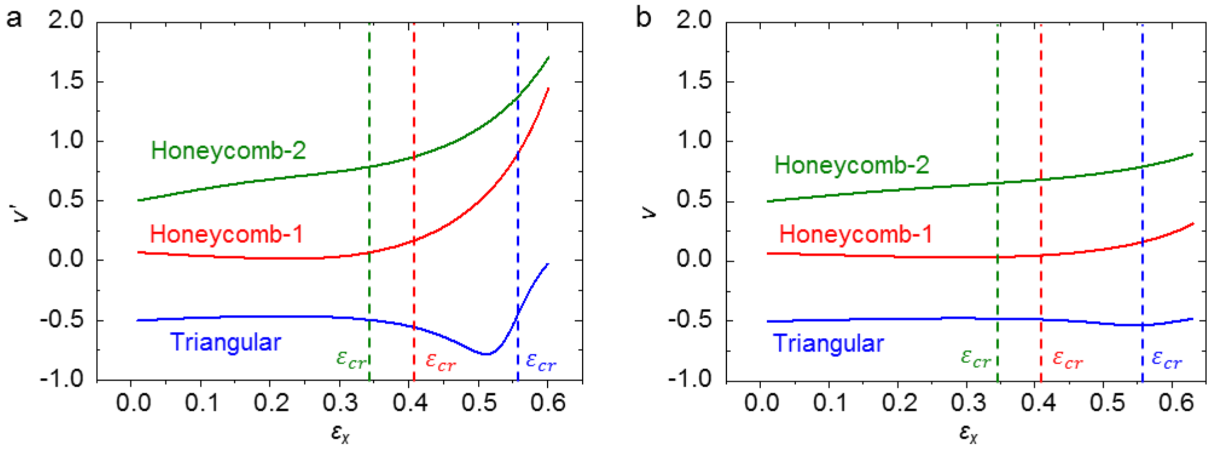

Figure S4. Schematic illustrations of theoretical model for an arbitrarily shaped curvy beam and triangular unit cells. (a) A simply supported beam microstructure subject to an axial force at the right end, and moments M_A and M_B at the two ends. The shape of microstructure is described by curvilinear coordinate (S). (b) An arbitrarily shaped curvy beam with or without a width reduction. (c) A pair of representative unit cells of triangular network materials subject to a uniform tensile stress along horizontal direction, with the free-body diagram of the horizontally aligned microstructure.

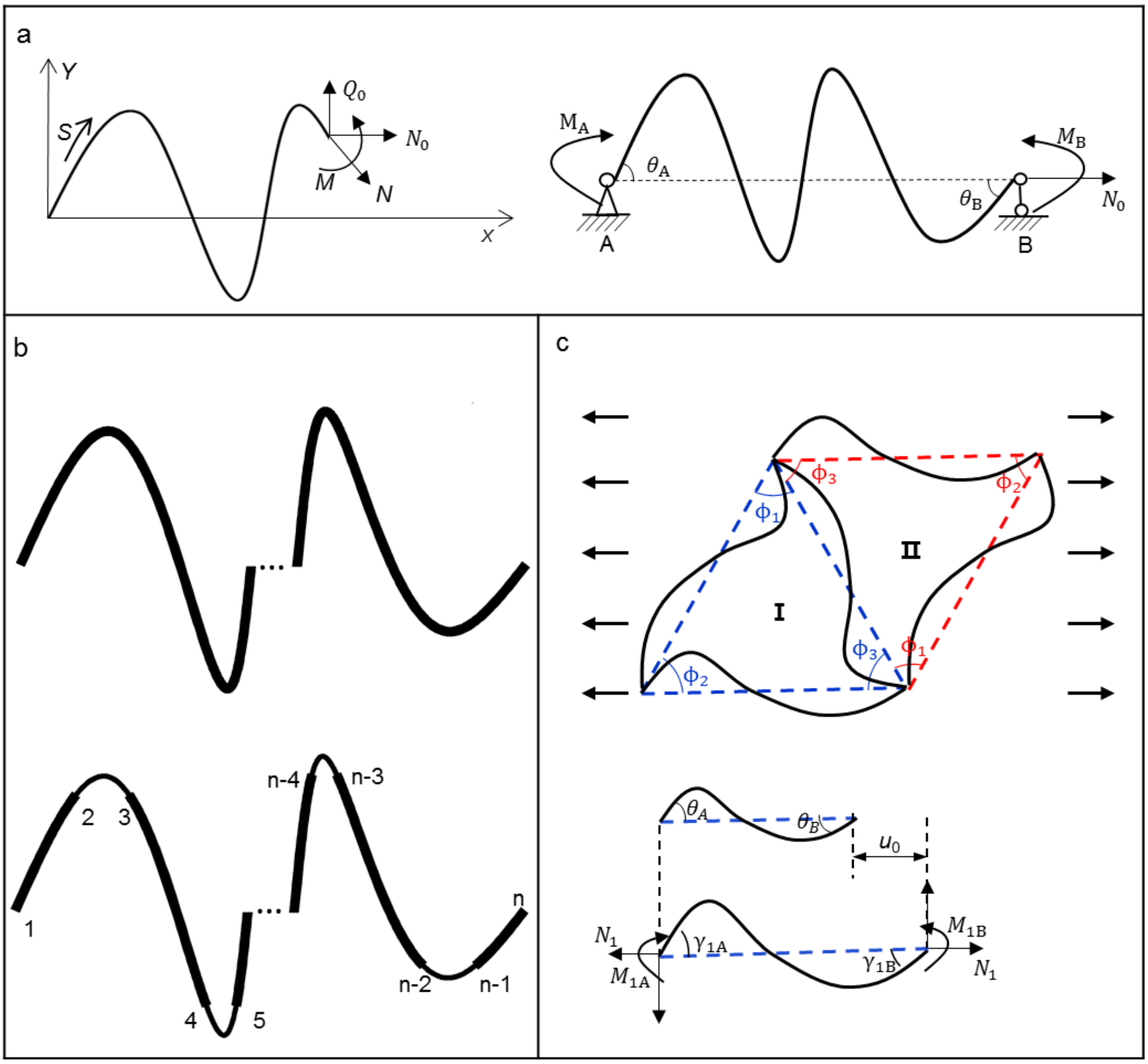

Figure S5. Geometric conditions of the normalized width ($\bar{w}$) and slopes ($\tan\theta_0$) that should be satisfied to form a triangular network material without any self-overlay. Here, the zigzag microstructure has no width reduction. The region below the solid line denotes the regime where the geometric conditions are met.

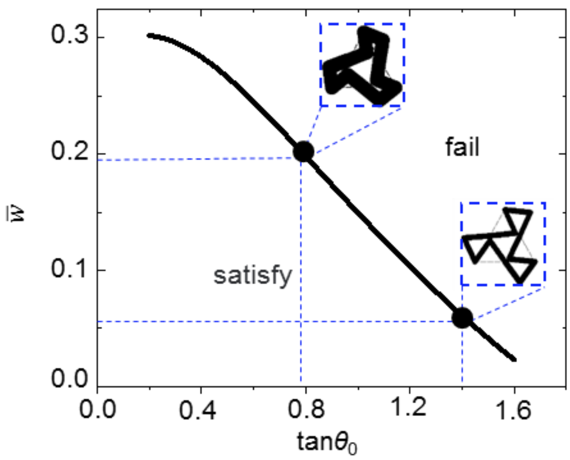

Figure S6. Linear Poisson's ratio (v) of triangular network materials versus the microstructure slope ($\tan\theta_0$) for a range of unit number (n_T) of the zigzag microstructure and the width-to-length ratio ($\bar{w}$), in the condition of $w_2/w_1 = 1$.

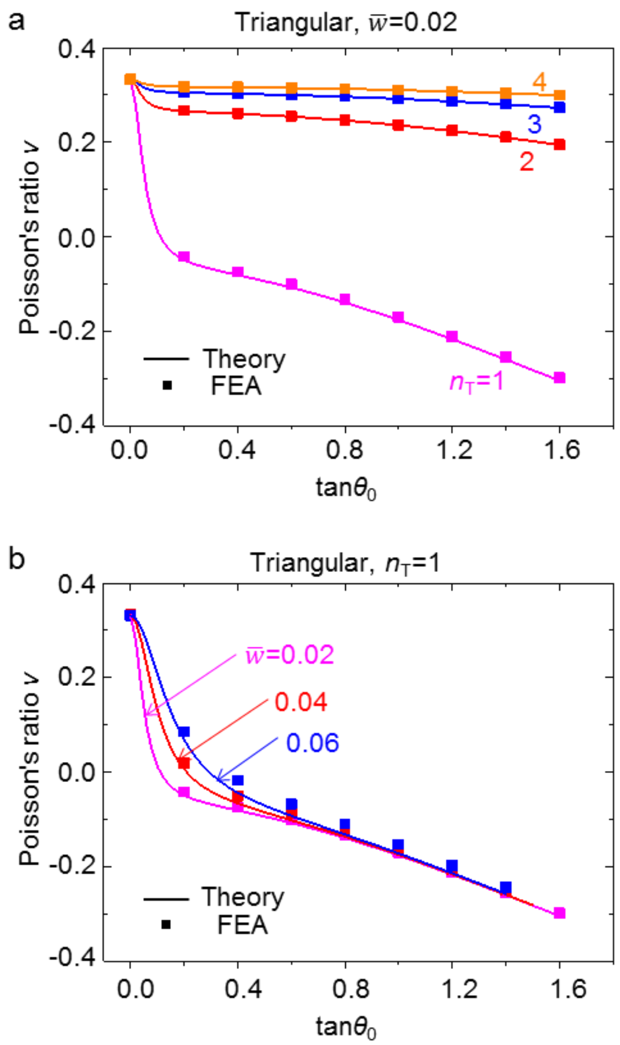

Figure S7. Theoretical and computational studies on the linear Poisson ratio of triangular network materials under infinitesimal deformations. (a) Linear Poisson's ratio (v) versus the width ratio (w_2/w_1) for a wide range of microstructure slopes ($\tan\theta_0$) and a fixed length ratio ($L_2/(L_1+L_2)$ = 0.1). (b) Linear Poisson's ratio (v) versus the length ratio ($L_2/(L_1+L_2)$) for a wide range of width ratio (w_2/w_1) and a fixed microstructure slopes ($\tan\theta_0$ = 1.0).

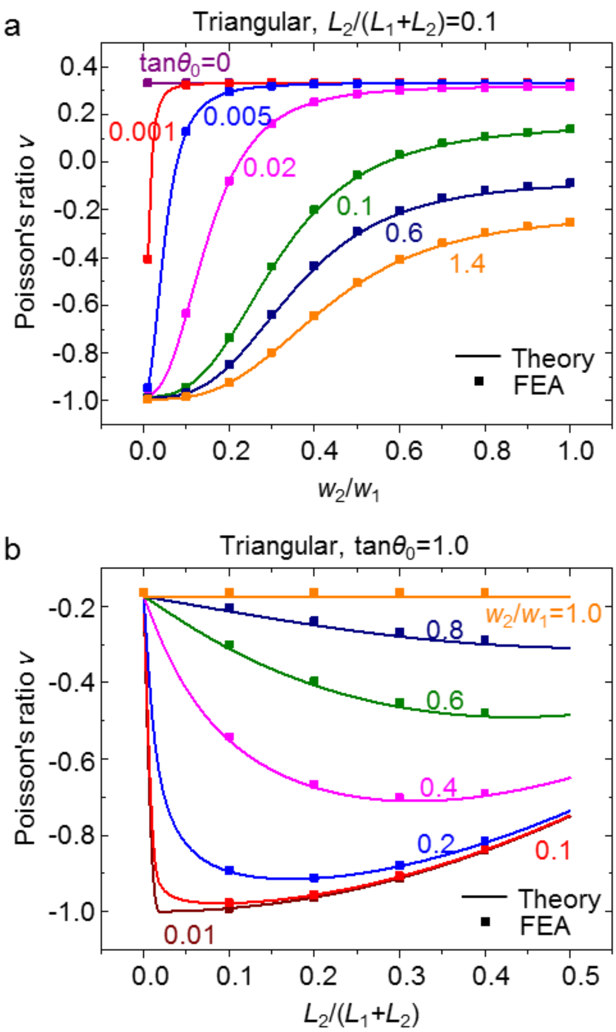

Figure S8. Microstructure slopes ($\tan\theta_0$) and width ratios (w_2/w_1) that yield zero linear Poisson's ratio (v) for four different length ratio ($L_2/(L_1+L_2)$ = 0.1, 0.2, 0.3 and 0.4) of triangular network materials (in **Fig. 3a**). The black solid line represents the curve fitted based on all of the dashed curves.

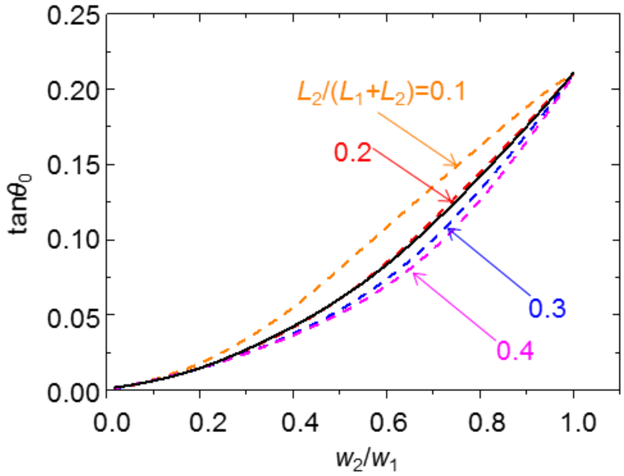

Figure S9. FEA results of triangular lattice materials under uniaxial stretching along different loading angles. (a) Poisson's ratio (v) versus the applied tensile strain (ε) along different loading angles (0°, 10°, 20°, and 30°) for the triangular network materials with $q = w_2/w_1 = 1.0$. (b)-(e) Similar results for network materials with $w_2/w_1 = 0.6$, 0.4, 0.2 and 0.1, respectively.

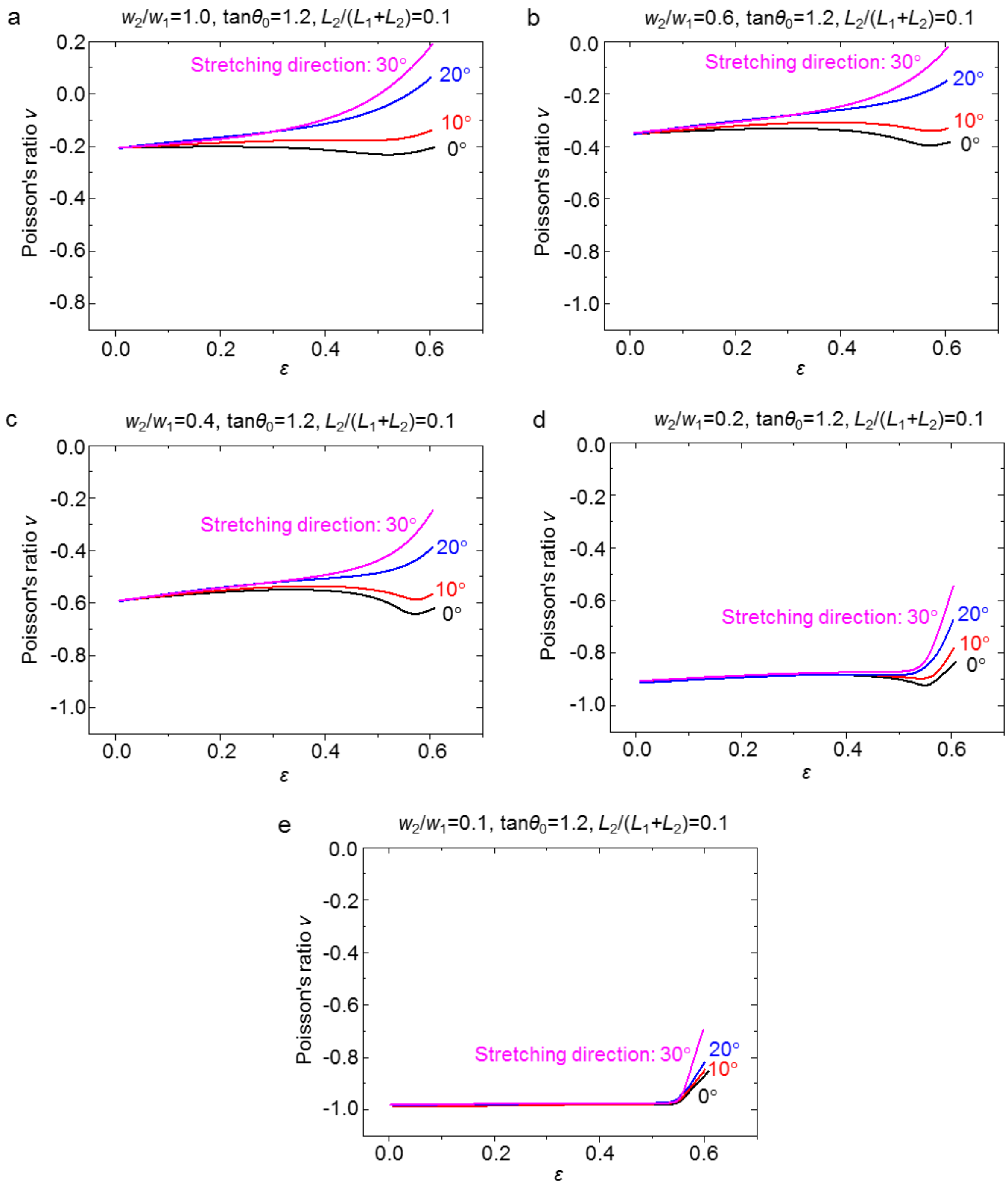

Figure S10. Critical strain (ε_{cr}) of the zigzag microstructure as a function of the microstructure slope ($\tan\theta_0$).

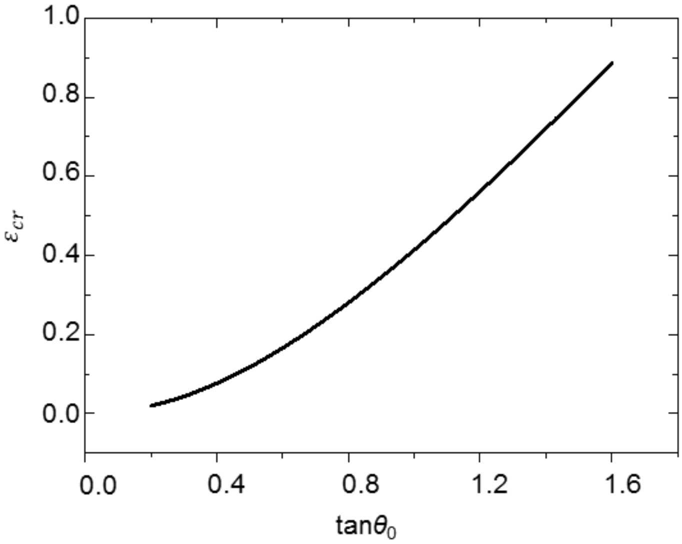

Figure S11. FEA images of the deformed configurations of triangular network materials under uniaxial stretching along vertical directions, with microstructure parameters: (a) $\tan\theta_0$ = 1.2, w_2/w_1 = 0.1, $L_2/(L_1+L_2)$ = 0.1, and (b) $\tan\theta_0$ = 1.2, w_2/w_1 = 0.6, $L_2/(L_1+L_2)$ = 0.1.

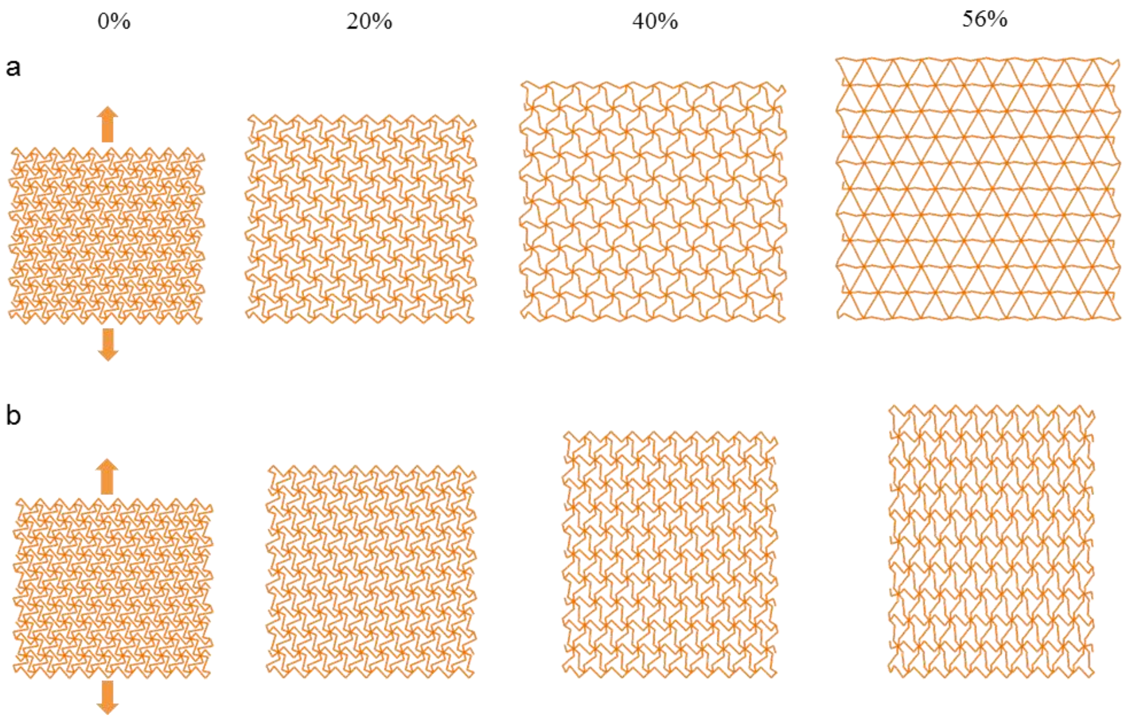

Figure S12. Maximum variation of Poisson's ratio $\Delta\nu$ for the applied strain ε_x increasing from zero to the critical strain ε_{cr} for different length ratios ($L_2/(L_1+L_2)$ = 0.1, 0.2, 0.3 and 0.4). The horizontal dashed line indicates $\Delta\nu$ = 0.05.

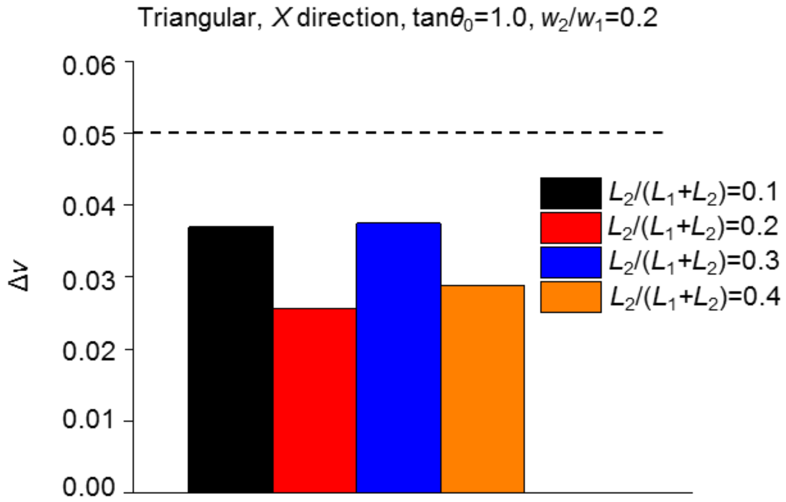

Figure S13. Maximum variation of Poisson's ratio $\Delta\nu$ for the applied strain ε_y increasing from 0 to $0.5\varepsilon_{cr}$.The horizontal dashed line indicates $\Delta\nu$ = 0.06.

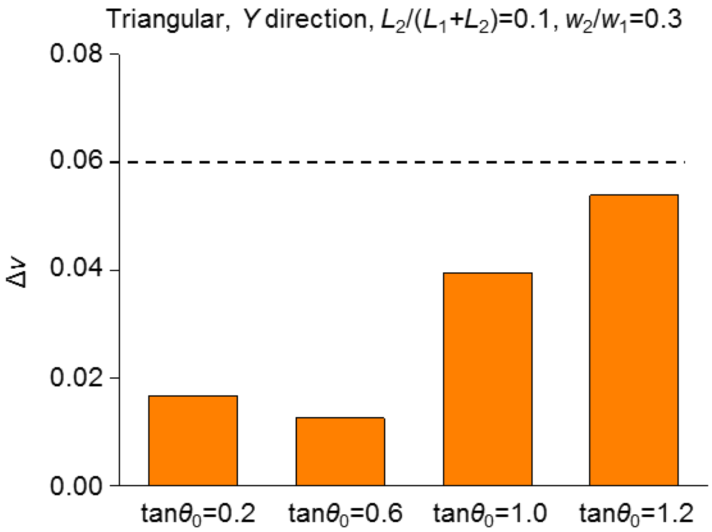

Figure S14. (a) Optical image for the as-fabricated artificial skin and schematic illustration of a unit cell. (b) Optical image for the artificial skin at the onset of fracture (~ 82% applied strain). Scale bar, 20 mm.

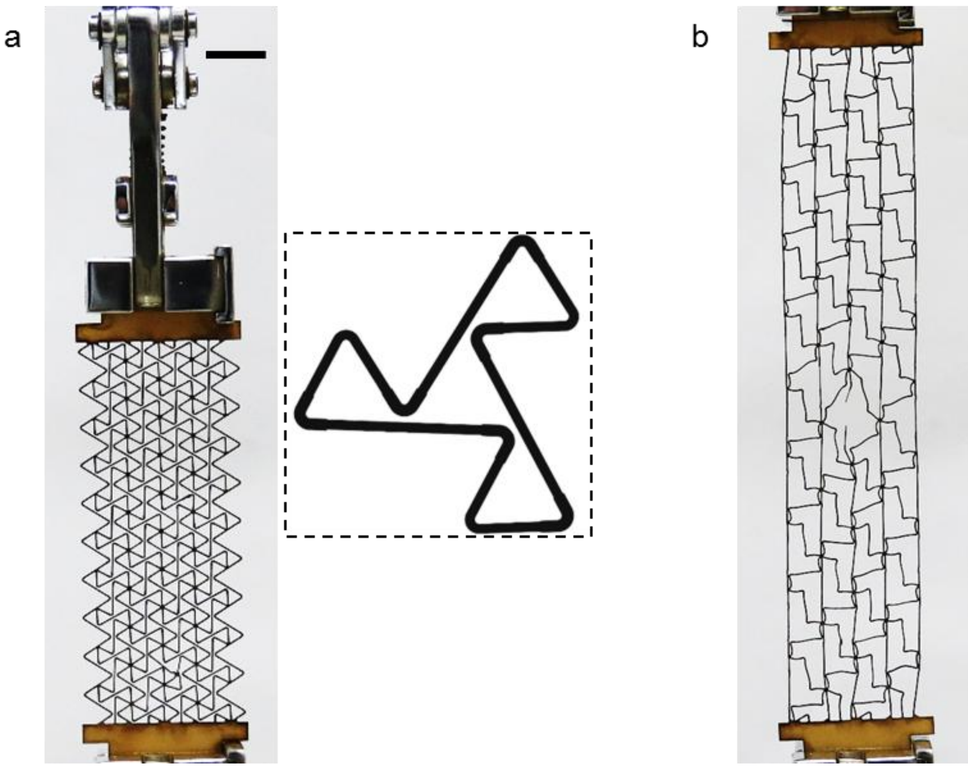

Figure S15. Theoretical and computational studies on the linear elastic modulus of triangular network materials under infinitesimal deformations. (a) Normalized linear elastic modulus (E/E_s) versus the microstructure slopes ($\tan\theta_0$) for a wide range of width ratio (w_2/w_1) and a fixed length ratio ($L_2/(L_1+L_2)$ = 0.1). (b) Normalized linear elastic modulus (E/E_s) versus the length ratio ($L_2/(L_1+L_2)$) for a wide range of width ratio (w_2/w_1) and a fixed microstructure slopes ($\tan\theta_0$ = 1.0).

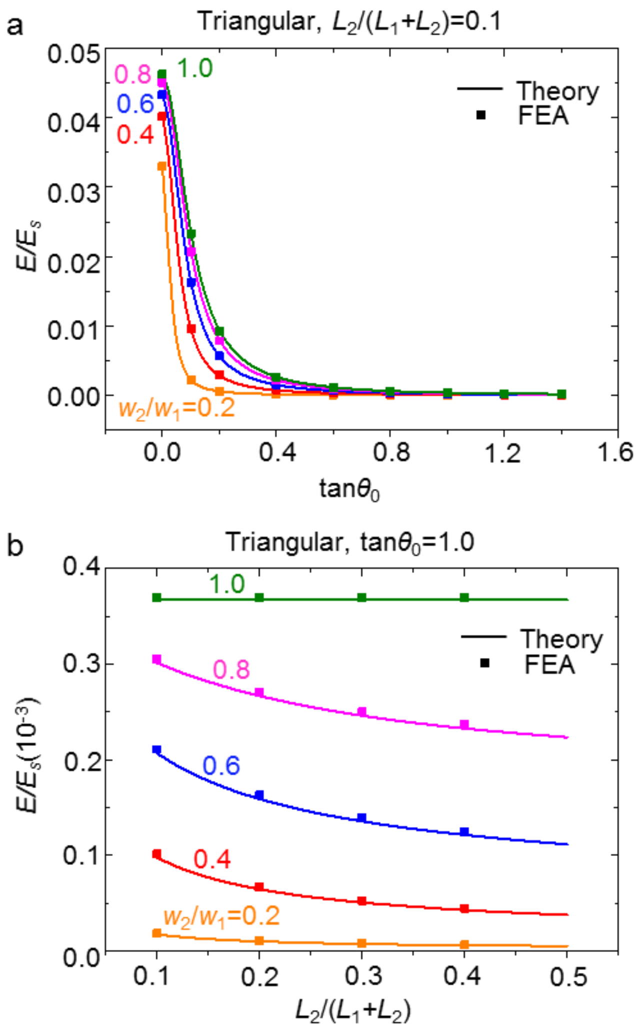

Figure S16. FEA results of stress-strain curves and tangent modulus-strain curves for the triangular network materials under horizontal stretching. (a) and (b) Stress-strain curves and tangent modulus-strain curves for the triangular network materials in **Fig. 5a**. (c) and (d) Similar results for the triangular network materials in **Fig. 5b**. The dashlines denote the critical strain (ε_{cr}) of the zigzag microstructure.

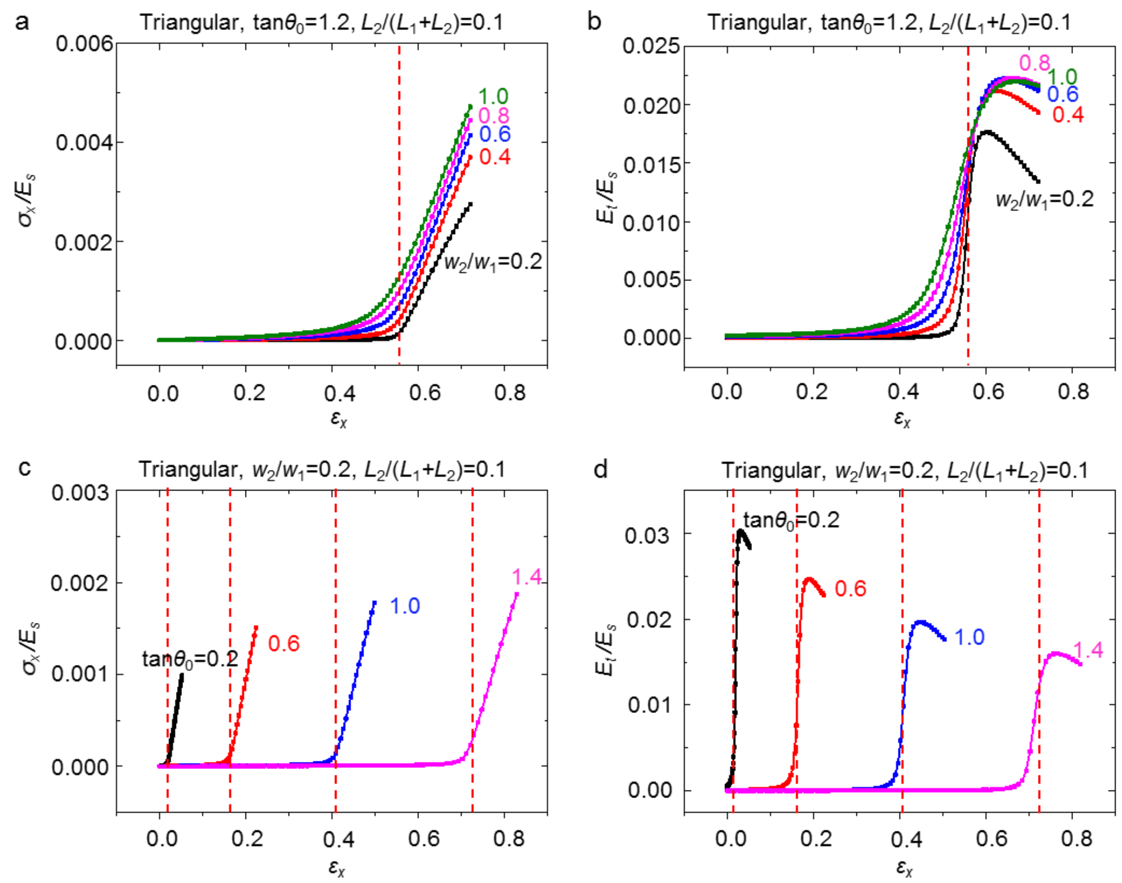

Movie Captions

Movie S1. This video illustrates synchronized experimental and computational results on the deformation processes of three network materials (with negative, 'zero' and positive Poisson's ratios) under uniaxial stretching (50%).

Movie S2. This video illustrates an architected cylindrical shell under axial compression and tension. It consists of three segments that possess negative, 'zero' and positive Poisson's ratios.